Boosting the Efficiency of Organic Solar Cells by Tuning the Optoelectronic Properties of Fluoranthene based Hole Transport materials via End Group Modification Technique

[1]Arifa Murtaza, [1]Ijaz Ahmad Bhatti, [1]Javed Iqbal* and [2]Muhammad Yaseen
[1]*Computational and Theoretical Lab, Department of Chemistry, University of Agriculture, Faisalabad 38000, Pakistan.*
[2]*Electronic Materials Lab, Department of Physics, University of Agriculture, Faisalabad 38000, Pakistan*.
javedkhattak79@gmail.com*

(Received on 2nd September 2025, accepted in revised form 11th April 2026)

Summary: To explore the photovoltaic and optoelectronic properties, a series of distinct para-substituted triphenylamine-based five-donor molecules (FBA1-FBA5) has been designed. The results show that the designed chromophores exhibit excellent effectiveness, with the highest red shift in the absorption spectrum, which entails appropriate photophysical attributes, high solubility, and a lower HOMO-LUMO energy gap (as a consequence of ionization potential), compared to the reported reference (**FBR**). The results ensure that the appropriate adjustment of the HOMO levels of HTMs enables the reduction of an energy barrier at the interface of an HTL and an ETL that injects a high hole vaccination and transportation rate. On the other hand, appropriate adjustment of the LUMO level prevents an electron leak from the electron transport layer (ETL) into the HTMs. Moreover, higher dipole moment, low reorganization energy and comparable estimated open circuit voltage (V_{OC}), make all freshly formulated molecules an efficient insight for fabrication of HTMs in perovskite and donors for organic solar cells for device working efficiency.

Keywords: Fluoranthene, HTMs, A-π-D-π-A framework, End group modification, third generation SCs, Optoelectronic properties and PCE measuring parameters.

Introduction

Renewable energy sources are promising substitutes that help to produce clean (without affecting ecological problems, *i.e*., greenhouse effect, global warming and air pollution) energy. To protect the earth from climate change, numerous efforts have been made to produce eco-friendly energy resources [23]. Certain highly deliberated renewable energy resources are geothermal, biogas [86], tidal [71], wind and solar energy [85]. Among these, solar energy is a commercial and environmentally friendly source of electricity. Solar cells are electronic devices that convert sun light into electricity. Silicon is the most common material used in the fabrication of (first generation) solar cells. These solar cells lead the market by 90% contribution worldwide. First generation solar cells were developed and reached about 180 µm of film thickness with high stability, long lifespan and a PCE of up to 26.64% [32, 43]. But they are associated with certain limitations, such as the ultra-pure semiconducting wafers being expensive due to complex manufacturing procedures [69]. The second generation of solar cells was based on gallium selenide, copper indium gallium selenide and cadmium telluride/cadmium sulfide material [60]. This photovoltaics based on CIGS have 20% power conversion efficiency, band gap (~1.7 eV), a life period of twelve years and a low price owing to less material consumption have some restrictions, *i.e*., lower power conversion efficiency and tremendous toxicity (*i.e*., Cd is toxic to the environment). Therefore, it is harsh to apply these solar cells to outfits, which has pushed the research community to explore alternatives [75].

The third-generation solar cells include perovskite and organic, which are constructed on the latest organic compounds [60]. Organic solar cells (OSCs) have the active layer, which is presented between the electrodes, that consists of a combination of donor and acceptor photoactive materials, which is the major harvester for sun light to decide the quality of materials and solar panel performance [7]. OSCs are an auspicious alternative candidate to overcome the inorganic solar generations owing to low cost [47], high flexibility [13], efficient visible light absorption and light weight with 10 nm of film thickness and have >20% PCE [78]. In addition, the large band gap and low PCE are major drawbacks of OSCs [64]. Recently, perovskite solar cells (PSCs) have attained much attention for both academic and the photovoltaic industry due to advantageous optoelectronic properties. These include low synthetic cost, excellent

*To whom all correspondence should be addressed.

charge mobilities, and light absorption in visible region with an absorption coefficient of 10-10 M-1 cm-1. Perovskite solar cells have shown remarkably high-power conversion efficiency (8 to 25.7%) [60] within a few years of their emergence, compared to other photovoltaic technologies [21, 41, 77]. Then, engineers focused on the composition engineering of electron transport and hole transport materials by using different fundamental methods to tune the optoelectronic and photovoltaic properties. For composition engineering of charge transport materials (electron and hole), several photoactive compounds *i.e*., conjugated polymers, oligomers and small organic molecules, are being used as donor and acceptor materials to enhance the PCE of third generation solar devices to fulfill the Shockley Queisser efficiency limit [75, 79].

The main challenge of HTMs is the requirement of dopants to achieve greater conductivity for attaining high PCE [27, 45]. However, the entire working efficiency of photovoltaic plans are hugely exaggerated by dopant supplies. The dopants not only compromise the reliability of perovskite solar cells, it also elevate the overall expenses. In short, the development of dopant-free hole transport materials (HTMs) is essential. The present scheme is focused on selecting appropriate dopant-free organic materials to tune the HTMs in solar cell appliances [90, 94]. By exploring a novel tri-phenylamine-based hole transport material has been selected from recent published literature [80]. The literature supports that the planner fluoranthene core-based HTMs have extraordinary potential to exploit in PSCs due to their auspicious electronic conformation and excellent charge transfer. These dopant-free hole HTMs are highly expected to offer PSCs with high power conversion efficiency and long-lasting robustness [74, 80].

In the current project study, we designed A-π-D-π-A type five HTMs (FBA1-FBA5) from the reported reference 4, 4-fluoranthene-3,8-diylbis(ethane-2,1-diyl)bis(N, N-bis(4-methoxy-phenyl) aniline (represented here as FBR) by modification of numerous light capturing terminal acceptor groups with a thiophene bridge . Here, A1 (2-ethylidene-malonitrile), A2 (5,6-difluoro 2-methylene-3-oxo-1H-inden-1-yildene malonitrile), 2-methylene-3-oxo-dicarbonitril (A3), 1-dicyanomethylene-2-methylene 3-oxo-indan-5,6-dicarbonitrile (A4), and methyl-2-cyanoacrylate (A5) terminal end-group acceptor units are integrated through a thiophene bridge on four sides of the TPA donor by replacing the methoxy group of reference. This molecular engineering amplifies intramolecular charge transportation among acceptor and donor units. The thiophene bridge unit and terminal acceptors can improve pi-pi stacking among the fluoranthene core and benzene ring of triphenylamine donor, and improve the charge transfer rate of the versatile core owing to effective charge delocalization. Moreover, the upsurge in conjugated backbone owing to integrated anchor electron-withdrawing groups and spacer have potential to adjust the energy levels. As a result, exceptional energy level placement reached a threshold value of 2.17eV with the light-absorbing perovskite film, which indicates that the fabricated HTMs revealed efficient hole extraction and transference characteristics. This study reveals prominent electronic coupling among the TPA donating unit and acceptor moieties, facilitating an exceptional 91% intrinsic charge, an appropriate photophysical profile (transparency in the visible portion λabs max< 700 nm), and improved power conversion efficiency, measuring attributes anticipated for derivative molecules. This research highlights its importance in proposing significant insights, strategies, and motivations for fabricating forthcoming state-of-the-art HTMs for perovskite solar cells.

Computational Methods

Geometry optimizations were performed using the Gaussian 9.0 [28] package and molecular structures were visualized with GaussView 5.0 [19] program. Density functional theory (DFT), a well-known method in computational chemistry, was employed for the evolution of the most realistic quantum mechanical characteristics, *i.e*., electronic as well as the vibrational parameters [33]. Initially, the ground state geometries of reported reference (FBR) were optimized at restricted spin by employing B3LYP [29], MPW1PW91 [24], CAM-B3LYP [59] and WB97XD [24] functionals with 6-31G (d,p) bases set using DFT. Among the tested functionals, *MPW1PW91/6-31G (d,p)* level of theory was selected as the most suitable method, because it provides the best agreement with the experimental wavelength of the reported FBR compound. All excited state simulations were performed both in the gas phase and in solvent using the polarizable continuum model (PCM) [34] combined with the time-dependent self-consistent field (TD-SCF) approach [25].

The UV-Visible spectra for the investigated molecules were generated by using Origin 6.0 Professional software [48]. Density of state spectra were generated using the PyMOlyze 1.1 software and transition density matrix analyses were performed with the Multiwfn 3.8 package [50]. The ground and

excited state geometries of neutral molecules (FBA1-FBA5) and their reorganization energies were computed for electrons (λ_e) and holes (λ_h) by using equations 1 and 2: [82].

$$\lambda_e = [E_-^0 - E_0] + [E_0^- - E_-] \quad (1)$$

$$\lambda_h = [E_+^0 - E_0] + [E_0^+ - E_+] \quad (2)$$

E_-, E_+ represent the anion and cation energies measured at -ve and +ve charge separately. These energy values were gained primarily by anionic and cationic geometries optimization and then additional imitations were done for energy calculations using negative and positive charges. E_0, $E_0^+$and E_0^- specify neutral, cationic and anionic ground state energies, respectively. E_-^0 and E_+^0 are ground state energies of anionic and cationic geometries of molecules [39, 61].

Results and Discussion

In this study, after careful assessment and comparison with experimental results, *MPW1PW91* functional is rationally chosen because its λ_{max} is observed at 468 nm, which justifies the closest agreement with the experimental value (473 nm) in literature, shown in fig. 2 (table 1S). Thus, *MPW1PW91* at 6-31G (d,p) level of theory is used for further calculations. The ChemDraw scheme of designed FBA1-FBA5 compounds crafted from FBR (reference) is depicted in fig. 1.

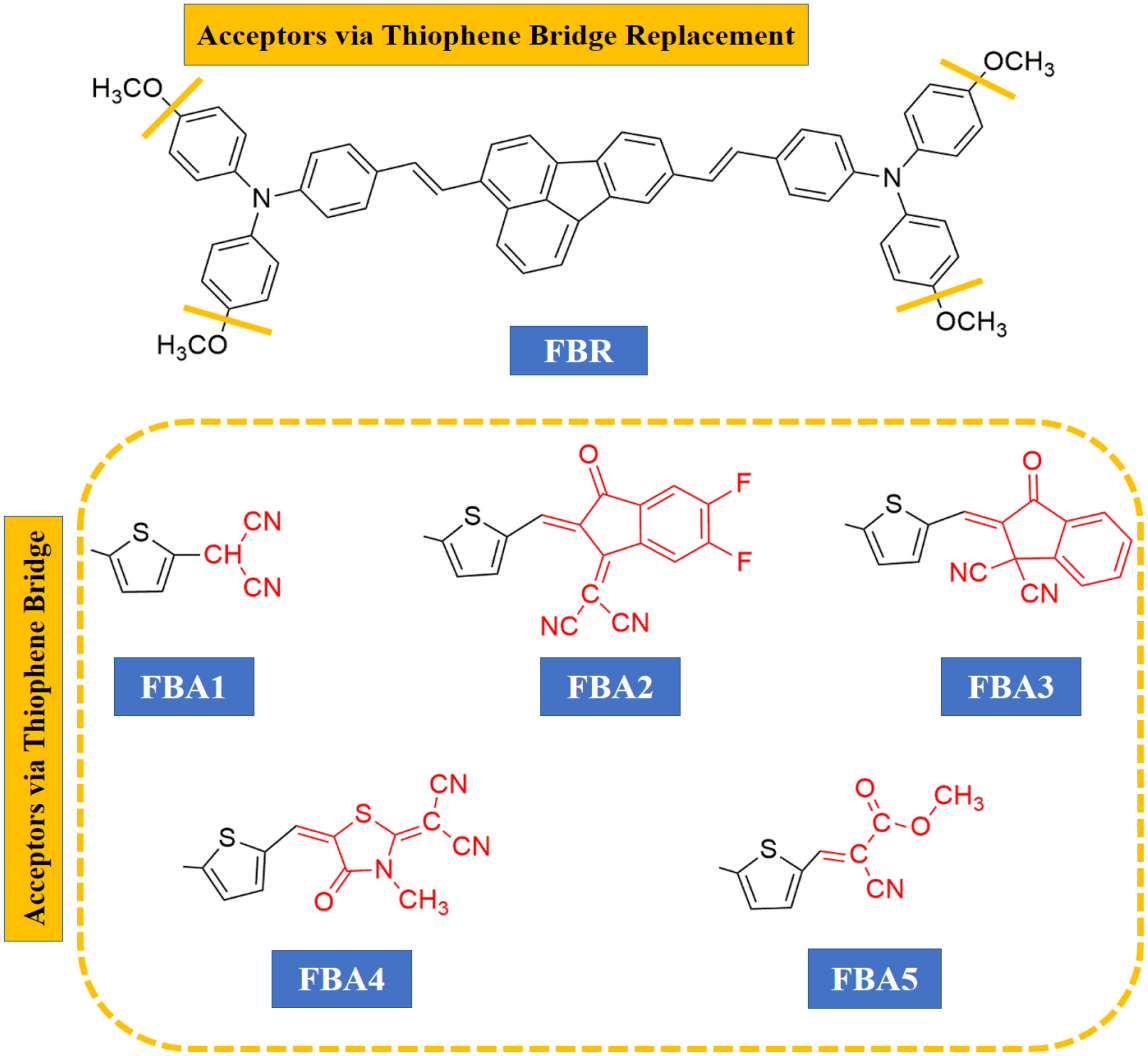

Fig. 1: Molecular schematic guidelines of newly designed FBA1-FBA5 HTMs crafted from reported FBR molecule.

Structural Optimization and Dihedral Angle

The optoelectronic properties of molecules have a strong relationship with ground state geometry optimization [72]. The degree of conjugation plays a critical role to improve an insight, specifically in the geometry of molecules. The planar structures have regular intra-molecular charge transfer and inter-molecular π-π stacking than others [95]. Some geometrical parameters, such as the bond length and dihedral angle, play an important role in analyzing the structural planarity. Dihedral angle has an inverse relationship to the structural planarity [68, 72, 88]. The optimized geometries of FBR and FBA1-FBA5 chromophores are shown in the figures. 3, containing fluoranthene core, TPA donor and thiophene as a bridge with terminal acceptor moieties. Enlisted bond length and bond angle values among different molecular fragments are described in table 1.

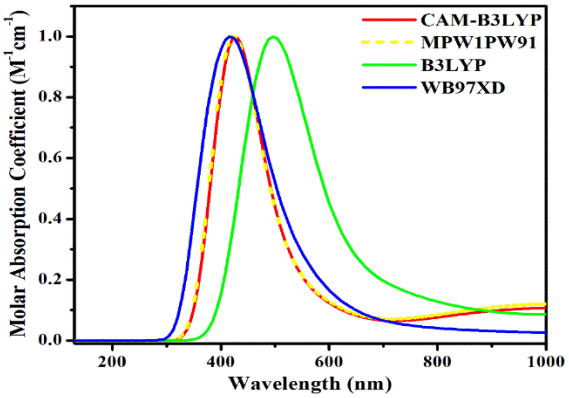

Fig. 2: Absorption spectrum of reference (FBR) with four distinct functionals.

Bond length of reference and all designed hole transport materials (HTMs) is 1.35-1.51 Å and the dihedral angle is ranging from 0.59° - 36.83° respectively. Here, d1 represents the bond length and θ1 the dihedral angle between donor-bridge, while d2 represents bond length between thiophene and end acceptor groups (θ2=dihedral angle between spacer via end acceptor groups). These results show that, bond lengths (d1 ranging from 1.35 to 1.46 Å and d2=1.40-1.51 Å) of all investigated molecules vary between (donor-bridge-acceptor) fragments. As we know, the single and double-bonded carbon atom bond lengths are 1.54 Å and 1.34 Å, representing the presence of conjugation that leads to good charge transfer and extended pi-pi stacking. Except for the FBA1 bond length (d2=1.51 Å), all HTMs depict the π-π stacking distance as small due to non-covalent interactions, *i.e.*, *S-π, N-N, F-F,* leading to better charge transfer via exaggerated conjugation.

Table-1: Bond lengths (Å) and dihedral angle (θ°) between the fragments of the reference molecule and their analogues.

Molecules	d1 (Å)	d2 (Å)	θ1 (°)	θ2 (°)
FBR	1.35	1.40	29.41	35.27
FBA1	1.46	1.51	28.01	18.67
FBA2	1.45	1.41	24.22	14.85
FBA3	1.46	1.42	24.01	5.48
FBA4	1.45	1.42	22.61	0.59
FBA5	1.45	1.42	36.83	0.94

Dihedral angle (θ1) of designed chromospheres is 28.01, 24.22, 24.01, 22.61, 36.83 degree. These results show that, except for θ1 (36.83°) of FBA5, all molecules hold nearly linear and planar configurations in optimized geometries of designed molecules as compared to FBR (29.41°) due to a small dihedral angle. Another hand, the θ2 (between bridge-acceptors) of reference is 35.27°. In this way, the θ2 (between bridge-acceptors) reduced values of FBA1-FBA5 donors are (0.59 < 0.94 < 5.48 < 14.85 < 18.67°) due to *S…O, S…N* intra-molecular connections and end-capped acceptor moieties modifications, which are more auspicious for conjugation and π-electron delocalization. Among all tailored molecules, FBA4 ensure the more planner optimized geometry and free rotation of a less sterically hindered terminal A4 (1-dicyanomethylene-2-methylene-3-oxo-indan-5,6-dicarbonitrile) fragment (connected to thiophene spacer) due to much decreased θ1 and θ2. Thus, the results illustrate that our designed donor molecules are exposing the coplanar 3D network packing structure. These (3D) grid structural modifications have offered supplementary electronic networks, excellent planarity through increased conjugation that leads to greater charge transmission, which boosts the power conversion efficiency of SC gadgets.

Optical Properties and Oscillator Strength

Oscillator strength is a dimensionless quantity that expresses the absorption ratio and emission of light radiation due to excitation of photons between two energy states [58, 81]. The light-harvesting efficiency (**LHE**) of molecules is directly related to oscillator strength (***f***). In demand to absorb higher molar absorption coefficient, we should increase the ***f*** of transition from ground energy state to high energy state [16, 42]. The oscillator strength is directly related to the square of its transition dipole moment ($\boldsymbol{\mu}$). Thus, a greater $\boldsymbol{\mu}$ directs the high oscillator strength, which indicates the stronger light absorptivity. Therefore, in order to attain ultra-strong near infrared response, strong electron-donating and electron-withdrawing groups are sandwiched to decrease the energy gap, in addition to increasing the $\boldsymbol{\mu}$ by increasing wave function overlay [87].

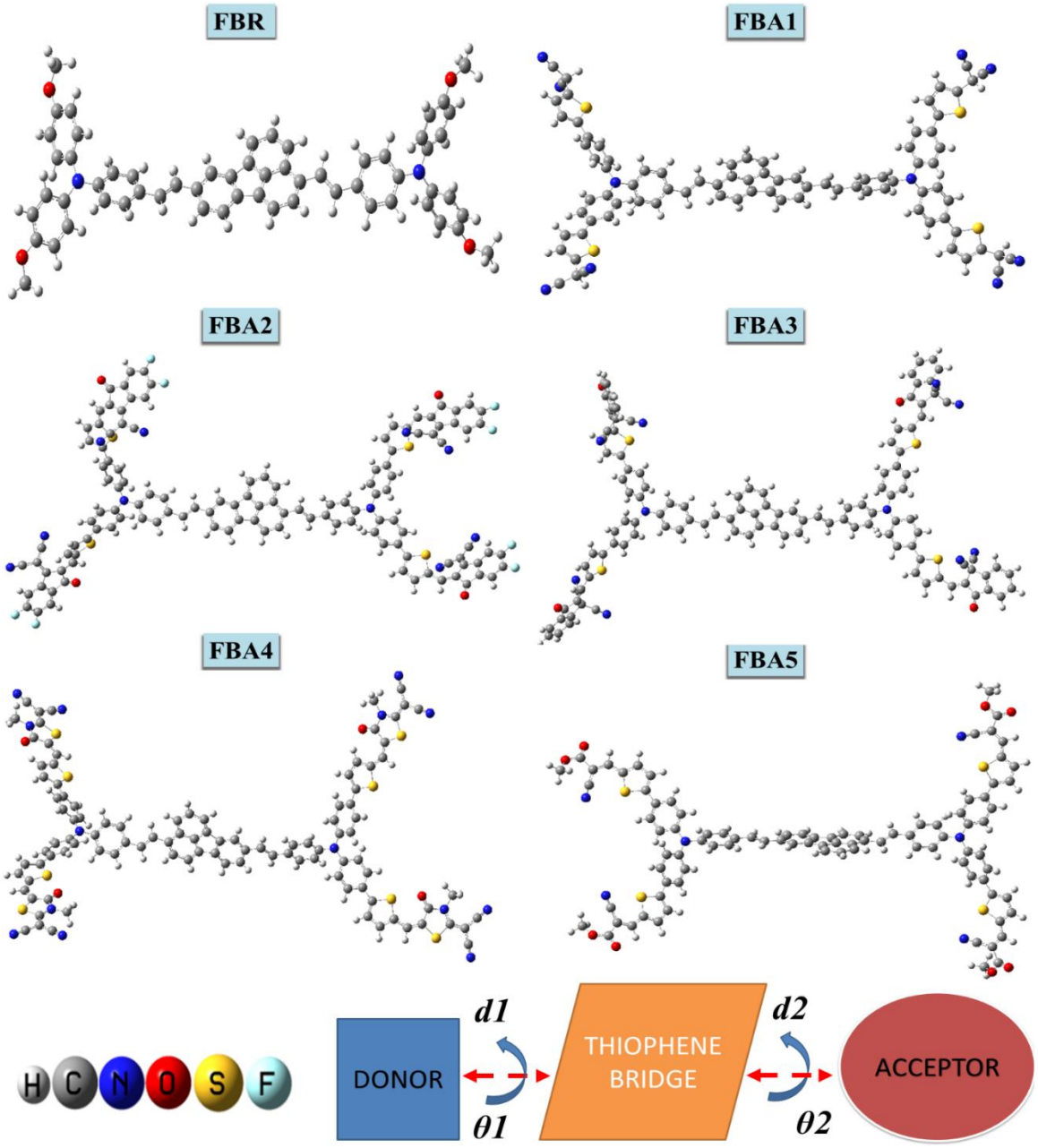

Fig. 3: Optimized geometries of FBR and tailored FBA1-FBA5 molecules at *MPW1PW91/6-31G (d, p)* level of theory.

UV-visible spectral study is a dominant factor to investigate the absorption characteristics of photovoltaic cells [30]. Photovoltaic properties analysis allows us to determine the energy levels, absorption coefficient and efficient charge carriage of small organic molecules (SOMs). These optical parameters boost the light capturing capability and PCE of organic photovoltaic (OPV) appliances [4, 27]. In order to above study, we employed strong auxochromic groups, *i.e*., sulphur (S), oxygen (O) and nitrogen (N) in structural modifications of new five non-fullerene (NF)/dopant-free donor molecules by taking as a reference (FBR) from the literature with acceptor-donor-acceptor architecture. To examine the light-harvesting assets of reference and freshly designed molecules, UV-visible spectra are computed with MPW1PW91 at the TD-DFT method by employing the IEFPCM model in solvent (dichloromethane) and gaseous medium.

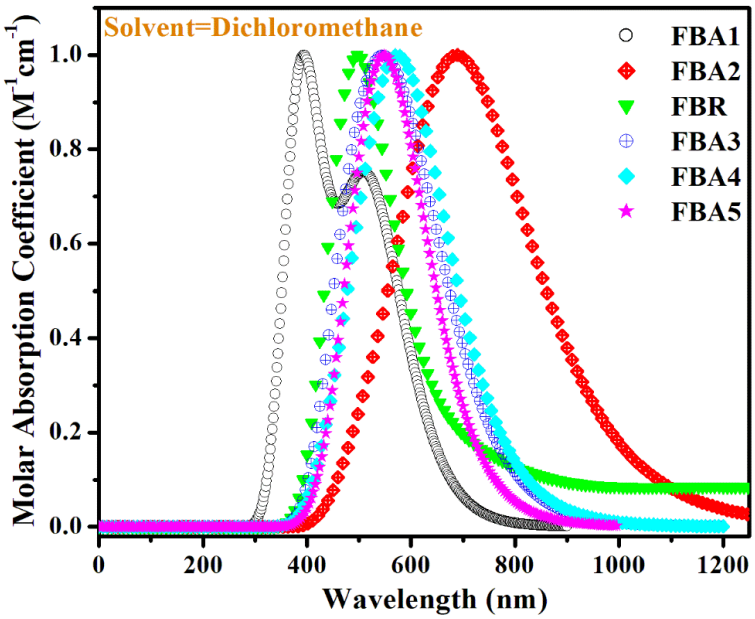

Fig. 4: Graph representing absorption maxima characteristics of FBR and designed compounds FBA1-FBA5 in dichloromethane.

The simulated absorption maximum values of FBR and designed (FBA1-FBA5) compounds in the gaseous phase are observed as 471, 500, 668, 579, 575, 531 nm respectively (fig. 5 and table 3S). The λ_{max} of reference FBR is 468 nm, 471 nm in the solvent and gas phase. In dilute dichloromethane, the theoretically computed light absorption value of FBR (468 nm) is closest to the λ_{max} value (473 nm) reported in the literature. The maximum wavelength, excitation energy, oscillator strength and transition character of model FBR and newly fabricated (FBA1-FBA5) chromophores in solvent medium are perceived in table 2S and fig. 4. Results illustrate that, all newly computed molecules have accompanied higher maximum absorption than the model molecule in dichloromethane. The λ_{max} values of crafted compounds lie in the range of 468-722 nm absorption and obey the following descending trend FBR (468 nm) < FBA1 (518 nm) < FBA5 (574 nm) < FBA3 (579 nm) < FBA4 (602 nm) < FBA2 (722 nm). So, the newly formulated (FBA1-FBA5) molecules have undergone the redshift owing to maximum absorption, strong electron withdrawing moieties, enhanced conjugation and energy levels modification that leads to greater oscillator strength via dipole moment in both gas and solvent media successfully. Moreover, FBA2, FBA3 and FBA4 compounds also exhibited higher λ_{max} due to electron-deficient end acceptor moieties. Therefore, the energy gap between HOMO-LUMO decreases and electron accepting efficiency of acceptor fragments due to sulphur, fluorine, cyanide and oxygen groups increases. The absorption maximum and reduced energy gap properties are best for the estimation of photovoltaic cells performance.

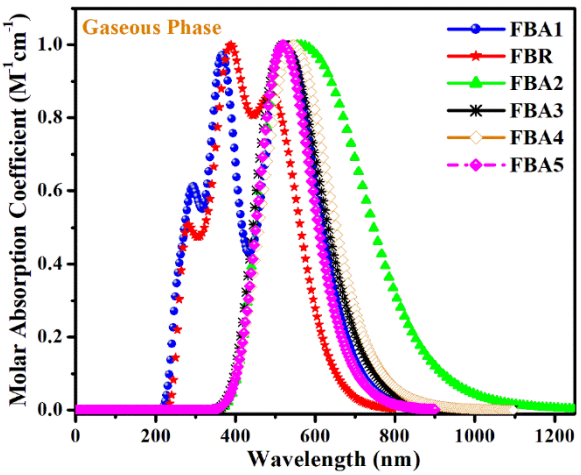

Fig. 5: Graph representing absorption maxima characteristics of FBR and FBA1-FBA5 molecules in gas phase.

Among all fabricated compounds, FBA1, FBA3 and FBA4 show the highest oscillator strength (2.20, 1.08 and 1.63) compared to the FBR (0.09) molecule in dichloromethane. In this way, the excitation energy of FBR (2.649 eV) and FBA1-FBA5 chromophores are 2.391, 1.715, 2.143, 2.059, 2.160 eV, respectively. On the other hand, the oscillator strength of FBR and all fabricated compounds are 0.09-2.17 range in a gaseous medium. Results

demonstrate that, the oscillator strength has a direct relationship with the light absorption and is inversely proportional to the excitation energy. Therefore, all sketched molecular electron withdrawing terminal substituent exhibits red shift in absorption spectra due to high *f* with low E_x than the reference (in both phases) and shift charge from core to end groups efficiently.

So, this project results revealed that, all scrutinized molecules have showed lowest excitation energy, the highest oscillator strength and λ_{max} in dichloromethane, which is a vital criterion for tuning optoelectronic properties of third generation solar cells. The lowest E_x and much higher *f* value of fabricated compounds in the solvent phase verify that, the freshly formulated chromospheres are solution processed and liable for amplified photo-current generation in perovskite and organic SCs.

Frontier Molecular Orbitals (FMOs)

Frontier molecular orbitals are the quantum mechanical descriptors that show an important part in understanding the optoelectronic attributes of photovoltaic cells [26]. Appropriate alignment of FMOs shows an important role in active charge abstraction from dynamic perovskite layers and the transference to produce photocurrent [54, 68]. Previous studies demonstrate that for efficient HTM in PSCs, the highest occupied molecular orbitals (E_H) of HTMs must be low-lying but should not surpass the valence band maximum of the perovskite layer (40, 92]. A low-lying and aligned (E_H) of hole transport materials is one of the main modules that influences open circuit voltage owing to the easier charge abstraction and effective transference [15, 76, 83]. In organic solar cells, charge carrying is done from acceptor LUMO to donor HOMO coupling for current generation which is collected inside the cell [3, 76]. The transportation of an electron from donor to acceptor is directly proportional to the efficiency of the device current and voltages. And this electron transfer is enriched by improving the electron excitation factor [20]. The band gap (E_g) can be calculated by equation 3 as:

$$E_{gap} = E_{L\,(LUMO)} - E_{H\,(HOMO)} \quad (3)$$

The HOMO-LUMO orbitals images of all compounds illustrate the charge transfer from the fluoranthene core by TPA donor to modified terminal acceptor moieties in red and green color fluffy balls (figs. 6) respectively. The energies of HOMO of scrutinized (FBA1-FBA5) molecules are -5.40, -5.54, -5.31, -5.53, -5.41 eV and while the energies of LUMO are -2.42, -3.37, -2.96, -3.09, -2.77 eV respectively. The reference molecule shows the HOMO energy -4.66 eV, while the LUMO energy is -1.88 eV. The HOMO of all FBA1-FBA5 (designed) chromospheres shows the charge accumulation more over the donor part and partially on the thiophene spacer while little to no charge distribution over the terminal acceptors, which is an indication of the good electron-donating nature of the HTMs. In circumstance of LUMO, FBR and FBA1 show charge spreading is denser over the central core while HOMO is entirely on the TPA donor unit except alkyl groups. In FBA2-FBA5 compounds, LUMO is concentrated totally on thiophene bridge and end acceptor groups. These concentrated charge distributions on central part are due to planner confirmation and lower charge spreading over alkyl groups is due to perpendicular substitutions of molecules. Among all fabricated molecules compared to the model compound, FBA2-FBA5 molecules' terminal fragments modification depict more dense LUMO energies -3.37, -2.96, -3.09, -2.77 eV. While the model compound (FBR) shows -1.88 eV of LUMO energy. The LUMO charge transfer of FBA2, FBA3, FBA4 and FBA5 is more concentrated on end-capped acceptors than HOMO, which indicates the strong electron-withdrawing capability of end groups due to the existence of nitro groups, which increase the conjugation effectively.

Table-2: Energy of orbitals and band gap of all molecules at *MPW1PW91* functional.

Molecules	E_{HOMO} (eV)	E_{LUMO} (eV)	E_g (eV)	IP	EA
FBR	**-4.66**	**-1.88**	**2.78**	**4.66**	**1.88**
FBA1	**-5.40**	**-2.42**	**2.98**	**5.40**	**2.42**
FBA2	**-5.54**	**-3.37**	**2.17**	**5.54**	**3.37**
FBA3	**-5.31**	**-2.96**	**2.35**	**5.31**	**2.96**
FBA4	**-5.53**	**-3.09**	**2.44**	**5.53**	**3.09**
FBA5	**-5.41**	**-2.77**	**2.64**	**5.41**	**2.77**

The H-L energy gap (E_g) of FBR is 2.78 eV and all FBA1-FBA5 designed molecules show 2.98, 2.17, 3.35, 3.44, 3.64 eV respectively (shown in table 2). FAB2, FBA3, FBA4 and FBA5 molecules are exhibiting the lowest energy gap (2.17, 2.35, 2.44, 2.64 eV) between the H-L as compared to FBR (2.78 eV) owing to vigorous electron withdrawing consequence of acceptors. The energy gap order of the investigated molecules in decreasing way are as follows: FBA1 > FBR > FBA5 > FBA4 > FBA3 > FBA2. This decreasing order of studied compounds signifies that the used end capped acceptors are responsible for reduced E_g. Band gap purposes the chemical reactivity, stability and power conversion efficiency of modified molecules [55]. The molecules with the lowest band gap have less stability, high reactivity with greater light absorbance and charge movement [81].

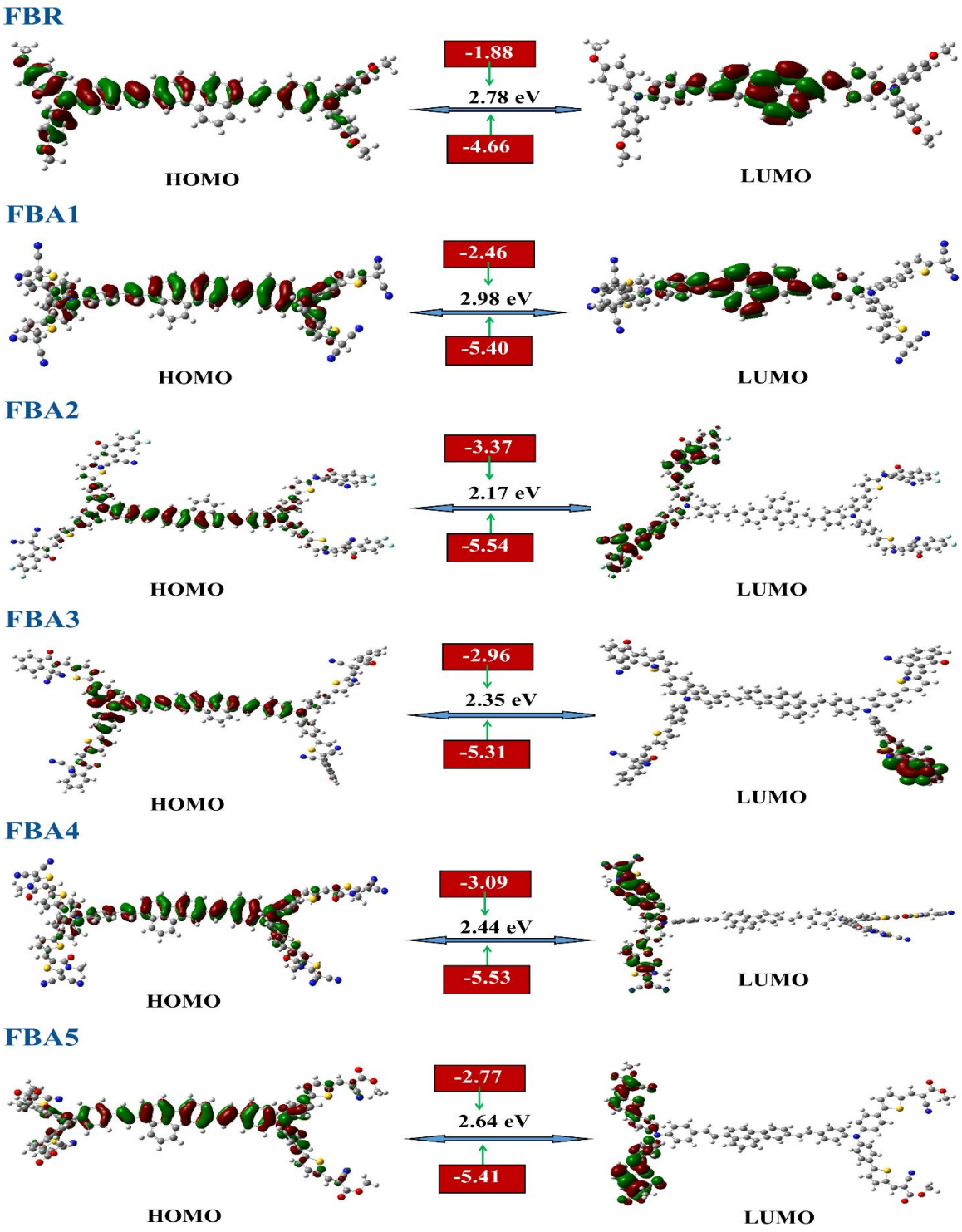

Fig. 6: Pictorial view of FMOs surface of optimized FBA1-FBA5 molecules.

Electron affinity (EA) and ionization potential (IP) are electronic parameters used to evaluate the charge moment nature of organic compounds. Ionization potential has an inverse relationship to the electron affinity [52]. The ionization energy (the energy required to move an electron from HOMO) demonstrates the electron-donating and accepting potential of compounds. High IP recommends stability, chemical inertness and while high reactivity is revealed by low ionization potential.

Electron affinity is the energy released when an electron is added to a ground state neutral molecule. Hence, a molecule attracts electrons easily if EA is high [61].

Surprisingly, in this project, all fabricated (FBR and FBA1-FBA5) compounds show higher electron affinity and lower IP value given in table 2. Thus, the charge transfer and lower IP value of all designed molecules as compared to the reported FBR molecule have proved the efficient electron-withdrawing nature of the acceptors. These chemical parameters can be measured by equations 4 and 5:

$$IP = -E_{HOMO\ VALUE} \quad (4)$$

$$EA = -E_{LUMO\ VALUE} \quad (5)$$

The given result shows that the studied molecules display excellent absorbance, a low band gap, and higher electron affinity, which improves the charge movement. These calculated outcomes supported the wisdom of molecular proposal of designed compounds for strong and broad band light absorption in OSCs and PSCs [36, 79].

Dipole Moment of Designed Donors

Dipole moment (μ) plays an important role in estimating the efficiency of PV gadgets by determining polarity, electron density and solubility of hole transport materials in organic solvents [64, 72]. The manufacturing mechanism of solar cells is significantly affected by the μ and is directly proportional to the solubility. The presence of a greater amount of polar auxochromic groups in small organic molecules is responsible for a greater dipole moment. Solubility of HTMs in organic solvents is higher due to the higher dipole moment [38]. The highly crystalline materials comprise a lower μ due to the cancellation of contrary dipole vectors creating a larger symmetrical structure. However, a greater dipole moment produced by asymmetric spreading of charge declared higher polarization (larger integer of polar atoms), which is auspicious for superior CT. Therefore, according to the 'like dissolves like' opinion, an increase in polarity will also improve the solubility of compounds in organic solvents [53, 82].

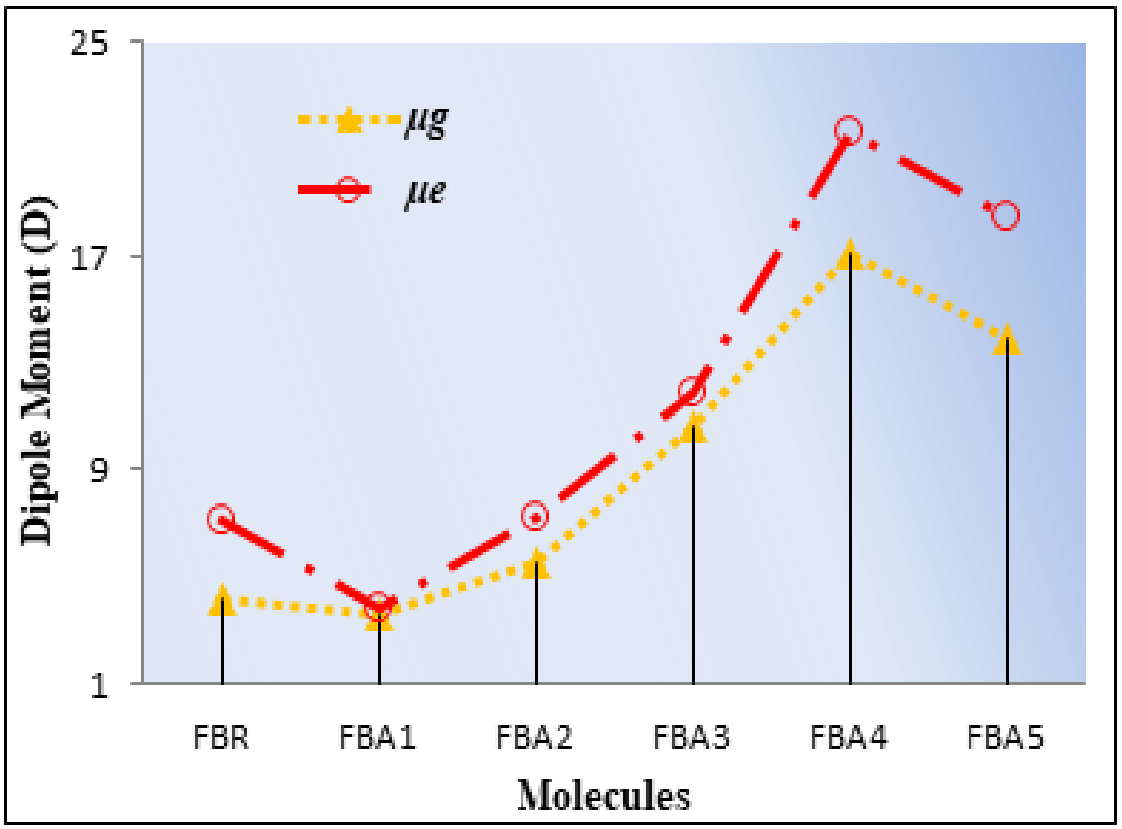

Fig. 7: Graphical outlook of dipole moment for FBR and FBA1-FBA5 compounds in solvent and gaseous phase with their difference.

In this study, the μ of the model (FBR) and fabricated (FBA1–FBAA5) compounds in the solvent and gaseous phases are computed using the TD-DFT method at *MPW1PW91/6-31G* level of theory. Systematically calculated dipole moment values and their difference of all studied molecules are listed in table 4S and its graphical representations portrayed in fig. 7. The μ of FBR in dichloromethane (μe) and gas phase (μg) is 7.115 D and 4.130 D. The dipole moment of designed molecules in solvent phase (μe) is 3.854, 7.096, 11.936, 21.677, and 18.499 D respectively. The ascending order of μg (gas phase) is in FBA4 > FBA5 > FBA3 > FBA2 > FBR > FBA1. Except for FBA1, the higher μ is observed for all scrutinized molecules in solvent and gaseous phases. According to μ simulations, the FBA2, FBA3, FBA4, and FBA5 compounds are much more cost-effective for solution-processed bulk-heterojunction SCs creation due to their higher solubility in dichloromethane, which reduces the hole-electron recombination. These outcomes propose that the freshly manufactured (FBA1-FBA5) molecules have greater solubility, self-arrange better charge mobility and excellent photovoltaic properties. So, in the future, these molecules will be preferred contestants in solar cell device fabrications.

Density of State (DOS)

Density of state study is performed to further authenticate the role of each moiety (bridge, donor and acceptor group) in creation of the absorption band and HOMO to LUMO orbitals. DOS is a systematic technique used to compute the number of states per energy levels by plotting a curve map theory (49, 57, 91). DOS analysis proves that, the varying electronic density as a function of different end-capped acceptors can alter the electron concentration of FMOs by Mullikan charge distribution theory [14, 18, 25].

Here, to investigate the density of state, the reported molecule FBR is fragmented into the core and the TPA unit. Same as reference, newly formulated HTMs are divided into bridge and acceptor by terminal modifications at *MPW1PW91/6-31G (d,p)* level of theory. Mullikan charge distribution of different fragments is arranged in table 5S. The high density of state values for architecture compounds represents various energy states. The zero value of DOS shows that no states exist for energy level activity. In DOS spectra, the donor is displayed in red, blue for core, purple and green lines exhibiting bridge and terminal acceptors. These graphs have the relative intensity on the y-axis and energy on the x-axis. In DOS graph, +ve values specify HOMO, while negative values demonstrate the LUMO and E_g is the band gap between valence and conduction bands. The relative peak intensities signify the existence of orbitals in separate segments of a molecule for charge movement.

Red, purple and green peaks highlight the maximum electronic cloud at the HMO-LUMO orbitals of TPA donor, the thiophene bridge, and acceptor unit. The red line peak intensity confirms the involvement of TPA donor towards HOMO in charge transfer shown in figs. 8. Fluoranthene core and TPA donor contributes 17.3, 82.7 % towards HOMO and 71.4, 28.6 % to LUMO. In FBA1-FBA5, acceptor contributes 14.8, 4.8, 3.8, 7.0, 3.9 % to HOMO and 17.3, 71.4, 85.9, 61.0, 56.0 % to LUMO respectively. Similarly, the percentage (%) contribution of bridge ranges from 6.5-21.8 towards HOMO and 1.3-28.0 to LUMO. DOS results validate the electronic density of thiophene bridge (B) and donor (TPA) towards HOMO for FBR, FBA1-FBA5, which is nearly the same raises form donor to end acceptor groups. The acceptor charge density towards LUMO is different for the entire designed compounds, reflecting that the lowest unoccupied molecular orbital has lengthy π links (conjugation) and efficient auxochromic groups. Among all, FBA2, FBA3 and FBA4 are exhibiting the highest percentage contribution of acceptor (71.4, 85.9, 61.0 %) in LUMO than other fragments, as indicated by a sharp and fine separated green line from the core peak, evidencing the greater charge transfer and excellent efficiency due to –CN and =O groups.

Reorganization Energy (RE)

Reorganization energy is computed to understand the charge mobilities (hole and electron) between the donor and acceptor moieties [11, 31]. Two types of reorganization energies are utilized to compute the effectiveness of scrutinized molecules of organic photovoltaics, namely internal reorganization energy and external *RE*. Mostly internal *RE* is considered because external *RE* is tough to estimate and is greatly underestimated for pure phase organic molecules [5]. So, here we have overlooked the external *RE*, and describe the internal reorganization energy (λin) of hole (λ_h) and electron (λ_e). Reorganization energy and charge transfer have an opposite relation with each other (Zara, Iqbal et al. 2017). Thus, if a molecule has low *RE*, has higher mobility of λ_e and λ_h. The λin of FBR and FBA1-FBA5 for hole and electron are calculated via equations 1 and 2 in table 3.

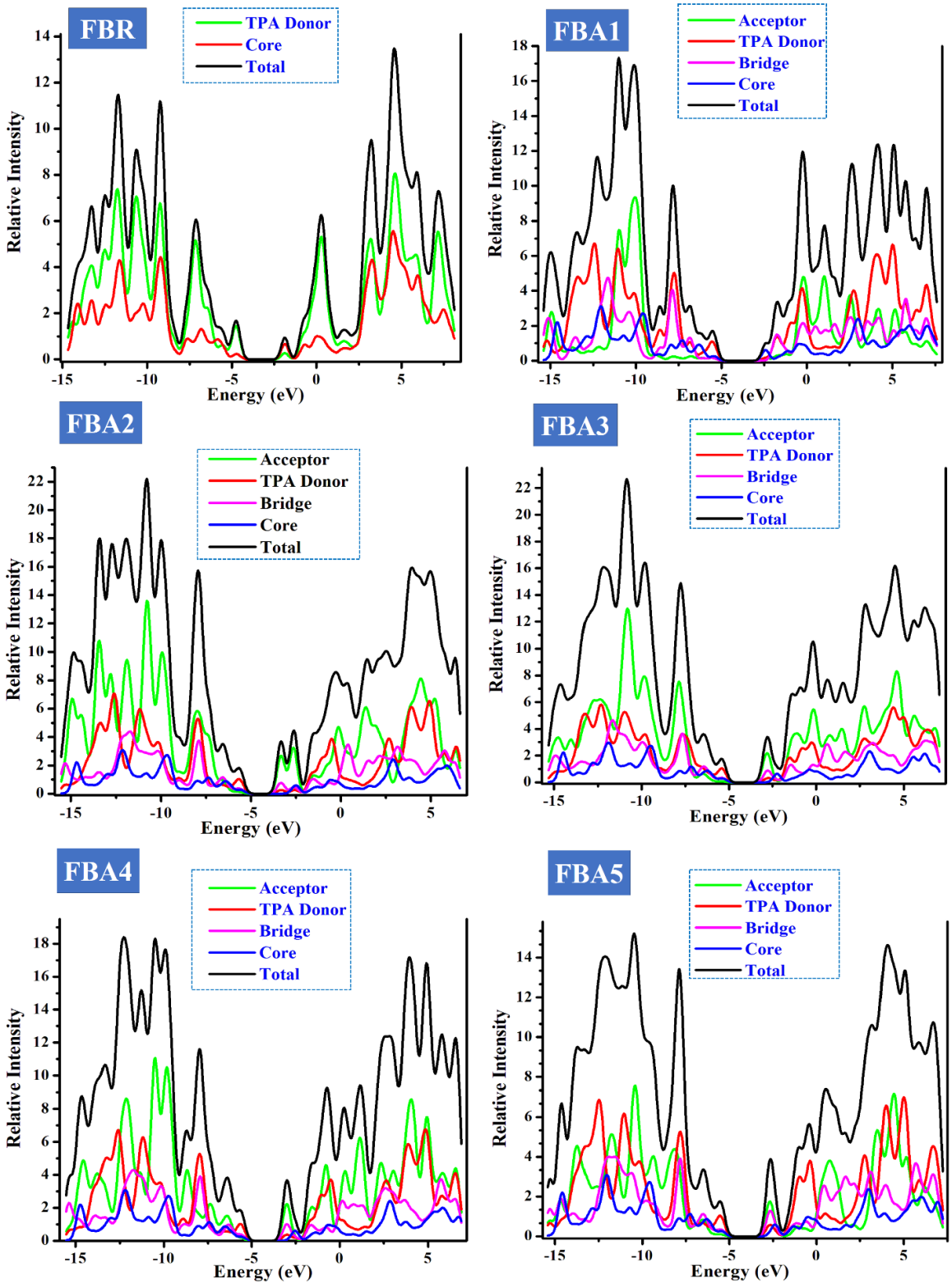

Fig. 8: DOS around HOMO-LUMO for FBR and FBA1-FBA5 chromophores.

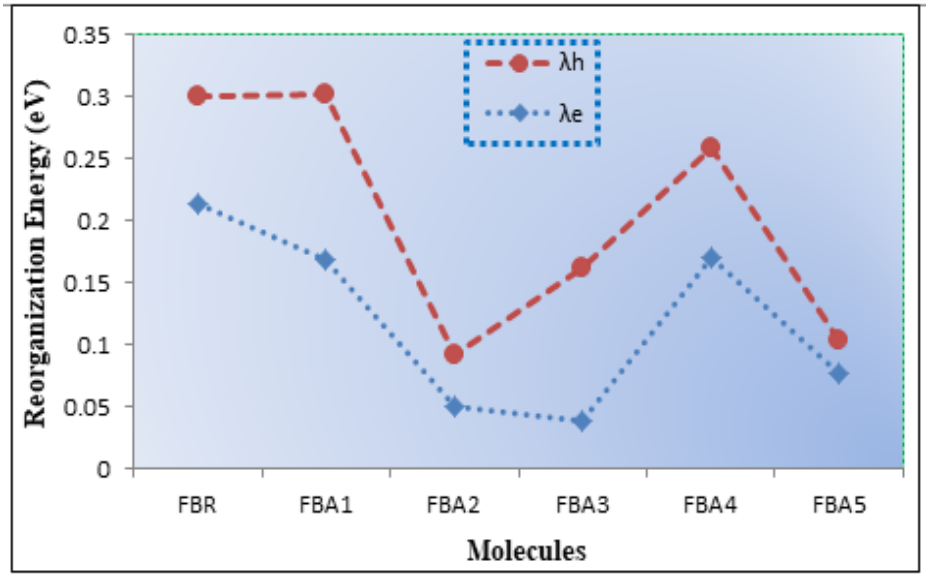

Fig. 9: The reorganization energy of λe and λh for FBR and FBA1-FBA5 compounds.

Table-3: Reorganization energy of reference with their analogues.

Molecules	λ_e (eV)	λ_h (eV)
FBR	**0.2139**	**0.0871**
FBA1	**0.1685**	**0.1341**
FBA2	**0.0503**	**0.0418**
FBA3	**0.0379**	**0.1245**
FBA4	**0.1699**	**0.0895**
FBA5	**0.0767**	**0.0268**

The hole *RE* energy for FBR (0.0871 eV) and their analogues, calculated in the range of 0.0268-0.1341 eV, are shown in a graph. 9. The results demonstrated the higher rate of electron movement between acceptor and donor groups in all FBA1-FBA5 molecules by means of a lower value of λe as compared to FBR. On the other hand, the greater electron mobility is unveiled by all formulated compounds (except FBA1 and FBA3) make them excellent candidates for end groups in this research. So, FBA3 and FBA1 can be restructured because the modified terminal acceptors in these compounds have various electronegative atoms that push them out of plane by decreasing the electronic dynamics. The electronegativity of atoms affects the planarity and charge carrier mobilities [96]. Overall, lower electron-hole *RE* is attained in all sketched chromophores, which makes them outstanding charge transfer aspirants and attractive hole transport materials.

The results visibly showed that the internal *RE* is mostly obeys on terminal electron withdrawing groups. Therefore, modification of different end acceptor functional moieties can improve the rate of charge transport, but certain functional groups encourage the carriage of electrons rather than holes [9, 73]. Usually, the low *RE* and adjacent ***π-π*** piling of the acceptor part will tune the opto-electronic properties, which is the essential principle for manufacturing highly efficient organic solar cells [35, 89].

Transition Density Matrix and Exciton Binding Energy

The amount of energy required to harvest free charge carriers is determined by the difference of 1st exciton energy and the band gap, called the binding energy. Binding energy (Eb) is an essential parameter for determining the optoelectronic properties of organic and perovskite semiconductor devices [62]. Furthermore, binding energy is employed to estimate the electrostatic forces between the hole and electron pairs [3, 61]. Empirically binding energy of inspected molecules is calculated by equation 6:

$$Eb = Eg - Ex \quad (6)$$

The exciton binding energy of small organic molecules should be as low as possible to permit the dissociation of bound hole-electron (exciton) pair into separate charges. Binding energy is also directly related to the energy gap of orbitals, as the E_g changes, the binding energy changes and vice versa [65]. The binding energy of designed chromophores FBA1-FBA5 and reference in dichloromethane is comparable to one another (table 4) and obeys the following order: FBR (0.131) < FBA3 (0.207) < FBA4 (0.381) < FBA2 (0.455) < FBA5 (0.480) < FBA1 (0.589).

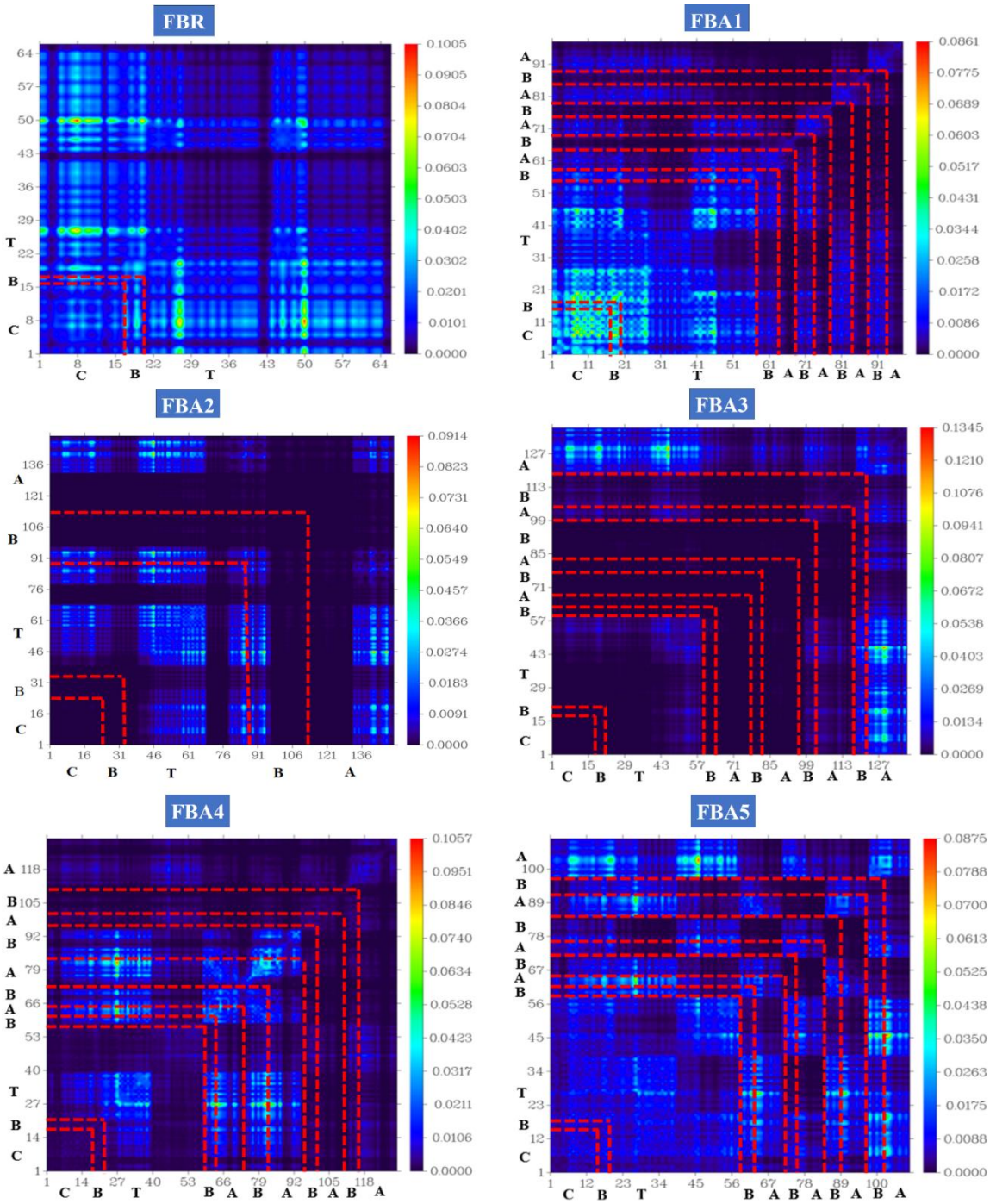

Fig. 10: The transition density matrix (TDM) plots of FBR and FBA1-FBA5 compounds.

Transition density matrix (TDM) is another implementation that is used for assessing hole-electron dynamics and a 3D map in excited state [37]. In an excited state, the transition density matrix support to clarify electronic excitation, D–A component interactions [8], electron-hole localization, delocalization diagonally and off diagonally [44]. As a consequence of tremendously limited influence on transitions in which we are interested, hydrogen atoms are excluded during TDM calculations [37]. Our reference and designed molecular structures are divided into three fragments: C for central core, TPA for the donor part, B for the bridge and A for terminal acceptor groups. Transition density matrix maps illustrate the visible effect of terminal groups on exciton detachment. Transition density matrix plots

provide the molecule's electronic density along the right axis and the atomic number along the bottom and left axes. The overall charge circulation in the model molecule is consistent, as shown in the TDM figs. 10. It is clearly seen from the results that FBA1, FBA2, FBA4, and FBA5 molecules have hole-electron coherence concentrates more on A and B units along the diagonal, off diagonally, revealing greater and easier charge migration from TPA donor part via bridge to terminal acceptors. According to TDM studies, newly designed compounds (FBA1-FBA5) are optimistic HTMs for PSCs and donor candidates for OSCs owing to their enhanced charge separation capacity in comparison to the reference.

Table-4: Calculated E_b, E_x and E_g values of reference and designed compounds in dichloromethane. All output files of entitled molecules accomplished via Gaussian 16.0.

Molecules	E_g (eV)	E_x (eV)	E_b (eV)
FBR	**2.78**	**2.649**	**0.131**
FBA1	**2.98**	**2.391**	**0.589**
FBA2	**2.17**	**1.715**	**0.455**
FBA3	**2.35**	**2.143**	**0.207**
FBA4	**2.44**	**2.059**	**0.381**
FBA5	**2.64**	**2.160**	**0.480**

Open Circuit Voltage (V_{OC})

Open circuit voltage is a parameter that plays a vital role in estimating the performance of the photovoltaic devices. The efficiency of PV devices is directly related to open circuit voltage [35, 81]. Open circuit voltage is the highest current that can be achieved from an electrical device when the applied voltage is zero [40]. Theoretically, V_{OC} is calculated by the difference of HOMO energy value of donor material and LUMO of acceptor molecule [2, 76]. In this work, we used Scharber and his colleague's equation 7 [70] for calculating the V_{OC} of reference and tailored molecules.

$$V_{OC} = E_{HOMO}^{Molecules\ (FBA1-FBA5)} - E_{LUMO}^{PC61BM\ (Acceptor)} - 0.3 \quad (7)$$

Various factors that affect the open circuit voltage, *i.e.*, dipole moment, light intensity source [10], device morphology [35], exciton binding energy and band gap [39]. Phenyl-C61-butyric acid methyl ester (PC61BM) is a well-known acceptor material used to compute the efficiency of organic and perovskite solar devices. Generally $\mathbf{V_{OC}}$ dependent on the HOMO and LUMO energies of donors and acceptors, respectively [51, 54].

The HOMO energies of our formulated donor molecules FBA1-FBA5, are directly aligned with the LUMO of *PC61BM* (acceptor) at selected functional (*MPW1PW91*). The HOMO-LUMO energy values of small organic molecules are shown in fig. 11 and table 9. The energy of LUMO of *PC61BM* is 3.70 eV and HOMO is 6.10 eV. The lower LUMO value of phenyl-C61-butyric acid methyl ester produces a larger open circuit voltage for improving the photovoltaic properties of organic and PSCs. Moreover, the energy gap (E_g) of designed donors (FBA1-FBA5) and acceptor molecules increases the PCE values of solar cells. Because the E_g of molecular orbitals from donor and acceptor materials increases directly as the V_{OC} of photovoltaic cells increases. The open circuit voltage value of *PC61BM* is different in all molecules, and totally depends upon the coupling donor materials. The V_{OC} values of FBA1-FBA5 compounds are 1.40, 1.54, 1.31, 1.53, 1.41 V, respectively, where the reference has an open circuit voltage of 0.66 V, which are comparable with each other. Open circuit voltage value of all designed chromophores with FBR is arranged in ascending way asFBA2 > FBA4 > FBA5 > FBA1 > FBA3 > FBR. In the present results, all newly fabricated molecules are exhibiting higher V_{OC} values as compared to reference. So, the given results reveal that all designed molecules are beneficial in revealing high power conversion efficiency in energy-deriving devices.

Light Harvesting Efficiency (LHE)

Light harvesting efficiency is the capability of compounds to produce charges within the conduction band by capturing light energy. Every photovoltaic material has the potential to generate charge carriers upon light absorption [46, 48, 84). According to **equation 8**, it is predicted that **LHE** and short circuit current (**J_{SC}**) are directly associated. If light harvesting efficiency rises, **J_{SC}** also rises and vice versa [66].

$$\boldsymbol{J_{SC} = \int_{\lambda}^{0} LHE(\lambda)\phi Inject \eta collectd\lambda} \quad \textbf{(8)}$$

In the above equation, ***φinj*** for electron injection, **LHE** for light harvesting efficiency and ***ηcollected*** stands for determined charge assembly. Theoretically, light harvesting effectiveness can be determined by employing an equation.

$$\boldsymbol{LHE = 1 - 10^{-f}} \quad \textbf{(9)}$$

Equation 9 "*f*" represents oscillator strength. Oscillator strength has a direct relationship with the LHE of molecules. In demand to absorb higher molar absorption coefficient, we should elevate the *f* of transition from the ground energy state to the high energy state [67]. Table 3, 4 denotes the calculated

light harvesting efficiency of all sketched molecules in the gas and solvent medium. The light harvesting efficiency of parent and designed molecules in the gas phase ranges from 0.109 to 0.993. Similarly, the decreasing trend of LHE values in dichloromethane is FBA1 > FBA4 > FBA3 > FBA5 > FBA2 > FBR. The light harvesting efficiency of reference FBR in the solvent and gaseous phase is 0.187. Briefly, it is determined that, all formulated compounds represent higher LHE values of donors than the reference in both phases, except the FBA3 value (0.109) in the gaseous phase.

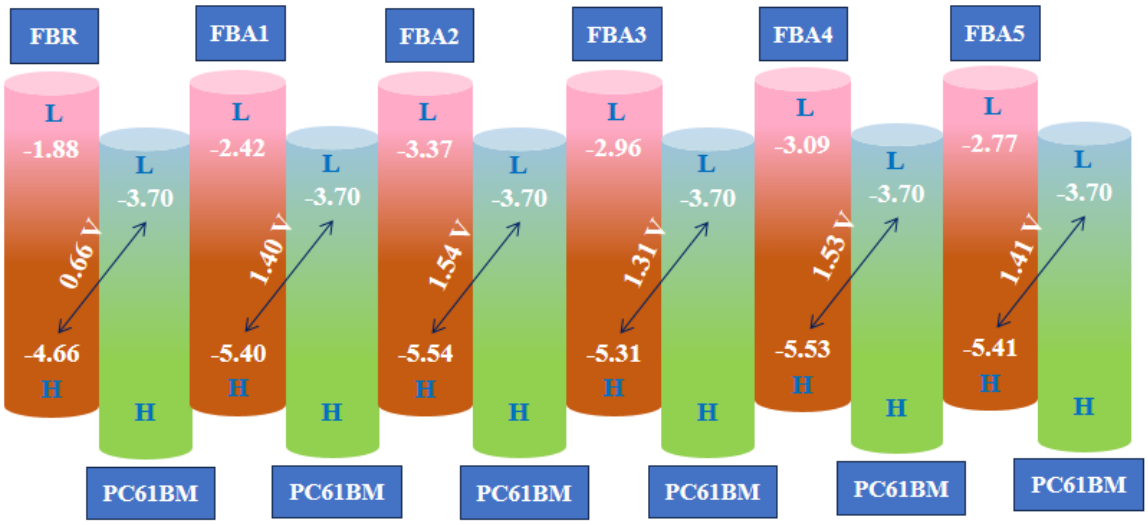

Fig. 11: Open circuit voltage value through HOMO of FBR and FBA1-FBA5 donor molecules with respect to LUMO of PC61BM acceptor.

Fill Factor and Power Conversion Efficiency

Fill factor (**FF**) is another alternative critical factor to calculate the **PCE** of solar cells, majorly depends on open circuit voltage values. A high fill factor characterizes the efficient solar cell. The given equation is used to compute the fill factor [1, 12, 22].

$$FF = \frac{eVoc}{KBT} - \frac{ln\left(\frac{eVoc}{KBT} + 0.72\right)}{\frac{eVoc}{KBT} + 1} \quad \textbf{(10)}$$

In equation 10, *eVocKbT* is the normalized V_{OC}, while *e* is a constant charge of one, *Kb* is the Boltzmann distribution constant having value 8.61733034105 $eVK^{-1}$and T is temperature (298 K). The computed FF values of reference and designed HTMs range from 0.8390 to 0.9258. All the newly sketched (FBA1-FBA5) small organic materials revealed a higher fill factor, endorsing the efficiency. Among all compounds, FBA2 and FBA4 compounds displayed the highest FF among all the calculated materials. This represents the extraordinary ability of FBA2 and FBA4 molecules to convert light energy into electrical energy and enhance the PCE functioning of photovoltaic devices. Results ensure that, all newly computed (FBA1-FBA5) chromospheres has highest fill factor with the increasing open circuit voltage.

Power conversion efficiency is a crucial parameter that enables the researcher to calculate the solar cell's efficiency and estimate economically how effectively the solar device can convert sun energy into electricity [63, 72]. To compute the power conversion efficiency of small organic molecules, **Voc**, $\mathbf{J_{SC}}$ and **FF** are important parameters. The power conversion efficiency of fabricated compounds is measured by employing equation [89].

$$PCE = \left(\frac{FF \times V_{oc} \times J_{sc}}{Pin}\right) \quad \textbf{(11)}$$

Pin represents the power of incident light, which is a stable quantity for all molecular units. Here, short circuit current (J_{SC}) is set as 22.32 mA cm^{-2}, experimentally measured for the reported reference (FBR) in literature [80].

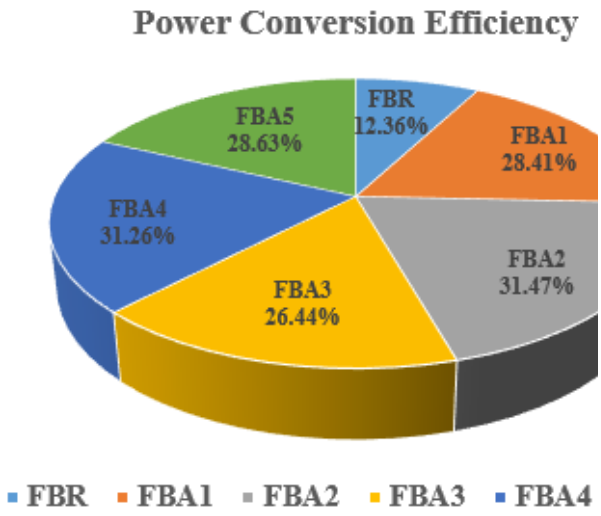

Fig. 12: Power conversion efficiency (%) pie chart of reference and designed compounds.

The results of power conversion efficiency measuring parameters (V_{OC}, J_{SC} and FF) for the investigated molecules are listed in table 6S. The results proved that the PCE (%) of all FBA1-FBA5 chromophores ranges from (12.36 to 31.47%) and following the ascending order, FBA2 > FBA4 > FBA5 >FBA1 > FBA3 > FBR. All designed molecules reveal a greater percentage of PCE as compared to the reference (12.36%) due to increasing FF and $V_{OC,}$ respectively. Graphical illustrations of power conversion efficiency are shown in Fig. 12. So, these outstanding project results suggest that all peripheral modifications in FBA1-FBA5 (designed) molecules are efficient. In the future, these donor materials can be used in the fabrication of photovoltaic devices to produce higher power conversion efficiency.

Conclusion

Up-to-date quantum chemical techniques were employed to study the effect of diverse terminal acceptor unit modifications of the tri-phenylamine-based materials (FBA1–FBA5) on the photovoltaic and opto-electronic properties. These freshly designed compounds have revealed red-shifted broad absorption spectra in the range of 518-722 nm in dichloromethane and 500-668 nm in gaseous phase while bearing lower excitation energy and reduced bandgap. The FBA2, FBA4 and FBA5 have demonstrated superior opto-electronic assets than FBA2 and FBA3 due to highly efficient auxochromic groups and extended conjugation of their external acceptors. Reorganization energies of all scrutinized chromospheres were calculated; the FBA2, FBA4, and FBA5 had high charge transfer with low electron (λ_e = 0.0503, 0.1699, 0.0767 eV) and hole (λ_h = 0.0418, 0.0895, 0.1267 eV) reorganization energy. The highest V_{OC} (1.41-1.54 V) values with respect to LUMO of PC61BM-HOMO donor have been detected for FBA1-FBA5; verify their capability to produce maximum current among entire compounds. It concluded that, the newly crafted molecules FBA1-FBA5, if applied in engineering energy driving solar devices, would display unlimited outcomes to enhance the power conversion efficiency. Hence, these end-capped acceptor modifications are an effective scheme for the fabrication of proficient next-generation photovoltaics. Therefore, FBA1–FBA5 compounds are highly endorsed to experimentalists to build more efficient SC devices.

References

1. A. Aboulouard, G. Gurek and M. El Idrissi, Computational study of organic small molecules based on imidazolinone for photovoltaic applications, Energy Sources, Part A, **43**, 2583–2594 (2021).
2. A. Aboulouard, S. Mtougui, N. Demir, A. Moubarik and M. Can, New non-fullerene electron acceptors based on quinoxaline derivatives for organic photovoltaic cells: DFT computational study, Synth. Met., **279**, 116846 (2021).
3. M. Adnan, J. Iqbal, S. Bibi, R. Hussain, M. N. Akhtar, M. A. Rashid and K. Ayub, Fine tuning the optoelectronic properties of triphenylamine based donor molecules for organic solar cells, Z. Phys. Chem., **231**, 1127–1139 (2017).
4. S. Ahmed and D. J. Kalita, End-capped group manipulation of non-fullerene acceptors for efficient organic photovoltaic solar cells: a DFT study, Phys. Chem. Chem. Phys., **22**, 23586–23596 (2020).
5. W. Akram, W. A. Zahid, L. A. El Maati, R. Altuijri, I. Hossain, M. S. Akhter and J. Iqbal, Engineering push–pull structural versatility in highly functional carbazole-based hole transporting materials design for efficient perovskite solar devices, J. Photochem. Photobiol. A Chem., **444**, 114991 (2023).
6. G. E. Alvarez, M. G. Marcovecchio and P. A. Aguirre, Optimization of the integration among traditional fossil fuels, clean energies, renewable sources, and energy storages: an MILP model for the coupled electric power, hydraulic, and natural gas systems, Comput. Ind. Eng., **139**, 106141 (2020).
7. K. Anagnostou, M. M. Stylianakis, K. Petridis and E. Kymakis, Building an organic solar cell:

fundamental procedures for device fabrication, Energies., **12**, 2188 (2019).
8. M. Ans, J. Iqbal, Z. Ahmad, S. Muhammad, R. Hussain, B. Eliasson and K. Ayub, Designing three-dimensional (3D) non-fullerene small molecule acceptors with efficient photovoltaic parameters, Chemistry Select., **3**, 12797–12804 (2018).
9. M. Ans, M. Paramasivam, K. Ayub, R. Ludwig, M. Zahid, X. Xiao and J. Iqbal, Designing alkoxy-induced based high performance near infrared sensitive small molecule acceptors for organic solar cells, J. Mol. Liq., **305**, 112829 (2020).
10. M. Ans, K. Ayub, X. Xiao and J. Iqbal, Tuning opto-electronic properties of alkoxy-induced based electron acceptors in infrared region for high performance organic solar cells, J. Mol. Liq., **298**, 111963 (2020).
11. S. Atahan-Evrenk and F. B. Atalay, Prediction of intramolecular reorganization energy using machine learning, J. Phys. Chem. A., **123**, 7855–7863 (2019).
12. U. Azeem, R. A. Khera, A. Naveed, M. Imran, M. A. Assiri, M. Khalid and J. Iqbal, Tuning of an A–A–D–A–A-type small molecule with benzodithiophene as a central core with efficient photovoltaic properties for organic solar cells, ACS Omega., **6**, 28923–28935 (2021).
13. S. Bati, Y. L. Zhong, P. L. Burn, M. K. Nazeeruddin, P. E. Shaw and M. Batmunkh, Next-generation applications for integrated perovskite solar cells, Commun. Mater., **4**, 2 (2023).
14. S. Bibi, R. A. Khera, A. Farhat and J. Iqbal, Triphenylamine based donor–acceptor–donor type small molecules for organic solar cells, Comput. Theor. Chem., **1198**, 113176 (2021).
15. M. A. Bilal. Siddique, M. Hussain, S. A. Siddique, M. Y. Mehboob, Z. Irshad, J. Iqbal and M. Adnan, Designing triphenylamine-configured donor materials with promising photovoltaic properties for highly efficient organic solar cells, Chemistry Select., **5**, 7358–7369 (2021).
16. J. A. Bjorgaard, K. A. Velizhanin and S. Tretiak, Solvent effects in time-dependent self-consistent field methods. II. Variational formulations and analytical gradients, J. Chem. Phys., **143**, 054102 (2015).
17. H. Chen, H. Liang, Z. Guo, Y. Zhu, Z. Zhang, Z. Li and Y. Chen, Central unit fluorination of non-fullerene acceptors enables highly efficient organic solar cells with over 18% efficiency, Angew. Chem., **134**, e202209580 (2022).
18. Z. Demircioglu, C. A. Kaştaş and O. Buyukgungor, Theoretical analysis (NBO, NPA, Mulliken population method) and molecular orbital studies of (E)-2-((4-hydroxy-2-methylphenylimino)methyl)-3-methoxyphenol, J. Mol. Struct., **1091**, 183–195 (2015).
19. R. D. Dennington, T. A. Keith and J. M. Millam, GaussView 5.0, Gaussian Inc., Wallingford., **20** (2008).
20. G. Deogratias, N. Seriani, T. Pogrebnaya and A. Pogrebnoi, Tuning optoelectronic properties of triphenylamine based dyes through variation of π-conjugated units and anchoring groups: a DFT/TD-DFT investigation, J. Mol. Graph. Model., **94**, 107480 (2020).
21. K. Devulapally, T. H. Chowdhury, Y. He, M. N. Rajesh, S. Prasanthkumar, A. Islam and L. Giribabu, Triphenylimidazole substituted D–π–D porphyrin based dopant-free hole transport materials for perovskite solar cells, J. Photochem. Photobiol., **16**, 100188 (2023).
22. J. Dhilipan, N. Vijayalakshmi, D. B. Shanmugam, R. J. Ganesh, S. Kodeeswaran and S. Muralidharan, Performance and efficiency of different types of solar cell material: a review, Mater. Today: Proc., **66**, 1295–1302 (2022).
23. L. Duan, Y. Chen, J. Yuan, X. Zong, Z. Sun, Q. Wu and S. Xue, Dopant-free X-shaped DA type hole-transporting materials for pin perovskite solar cells, Dyes Pigm., **178**, 108334 (2020).
24. A. Dwivedi and A. Kumar, Molecular docking and comparative vibrational spectroscopic analysis, HOMO–LUMO, polarizabilities and hyperpolarizabilities of N-(4-bromophenyl)-4-nitrobenzamide by different DFT methods, Polycycl. Aromat. Compd., **41**, 387–399 (2021).
25. A. Farhat, R. A. Khera, S. Iqbal and J. Iqbal, Tuning the optoelectronic properties of subphthalocyanine derivatives for photovoltaic applications, Opt. Mater., **107**, 110154 (2020).
26. R. Fatima, R. A. Shehzad, A. Rasool, M. Yaseen, S. Iqbal, M. J. Saif and J. Iqbal, Exploring the potential of tetraazaacene derivatives as photovoltaic materials with enhanced photovoltaic parameters, Int. J. Quantum Chem., **122**, e26817 (2022).
27. R. Fatima, J. Iqbal, S. Bibi and M. Yaseen, Exploring acceptor modification in helicene-phenylamine-based small molecules for organic and perovskite solar cells, Energy Technol., **12**, 2301019 (2024).
28. M. Frisch, Gaussian 16, Revision B.**01**, Gaussian Inc. (2016).
29. M. D. Ganji, S. M. Hosseini-Khah and Z. Amini-Tabar, Theoretical insight into hydrogen adsorption onto graphene: a first-principles

B3LYP-D3 study, Phys. Chem. Chem. Phys., **17**, 2504–2511 (2015).
30. M. Hachi, A. Slimi, A. Fitri, S. ElKhattabi, A. T. Benjelloun, M. Benzakour and M. Mcharfi, New small organic molecules based on thieno[2,3-b]indole for efficient bulk heterojunction organic solar cells: a computational study, Mol. Phys., **118**, e1662956 (2020).
31. S. Hameed, S. Gul, M. Ans, I. A. Bhatti, R. A. Khera and J. Iqbal, Designing Y-shaped two-dimensional polymer-based donor materials with addition of end group acceptors for organic and perovskite solar cells, J. Mol. Model., **29**, 152 (2023).
32. C. He, Z. Chen, T. Wang, Z. Shen, Y. Li, J. Zhou and H. Chen, Asymmetric electron acceptor enables highly luminescent organic solar cells with certified efficiency over 18%, Nat. Commun., **13**, 2598 (2022).
33. J. Hou, O. Inganäs, R. H. Friend and F. Gao, Organic solar cells based on non-fullerene acceptors, Nat. Mater., **17**, 119–128 (2018).
34. R. Improta and V. Barone, Absorption and fluorescence spectra of uracil in the gas phase and in aqueous solution: A TD-DFT quantum mechanical study, J. Am. Chem. Soc., **126**, 14320–14321 (2004).
35. M. Irfan, J. Iqbal, S. Sadaf, B. Eliasson, U. A. Rana, S. Ud-din Khan and K. Ayub, Design of donor–acceptor–donor type small molecule donor materials with efficient photovoltaic parameters, Int. J. Quantum Chem., **117**, e25363 (2017).
36. F. Jilani, J. Iqbal, I. Shahid, M. Yaseen, M. S. Mahr, M. Khalid and K. Ayub, Rational design of naphthalimide based small molecule non-fullerene acceptors for organic solar cells, Comput. Theor. Chem., **1187**, 112916 (2020).
37. J. W. Jung, J. W. Jo, C. C. Chueh, F. Liu, W. H. Jo, T. P. Russell and A. K. Y. Jen, Fluoro-substituted n-type conjugated polymers for additive-free all-polymer bulk heterojunction solar cells with high power conversion efficiency of 6.71%, Adv. Mater., **27**, 3310–3317 (2015).
38. N. Kanwal, R. Hussain, A. Sattar, M. A. Assiri, M. Imran, A. Hussain and T. Hassan, DFT based modeling of asymmetric non-fullerene acceptors for high-performance organic solar cells, Opt. Quantum Electron., **54**, 546 (2022).
39. K. Q. Kayani, U. Yaqoob, S. Jabeen, S. Iqbal, M. Yaseen, M. Khalid and J. Iqbal, Tris-isopropyl-sily-ethynyl anthracene based small molecules for organic solar cells with efficient photovoltaic parameters, Comput. Theor. Chem., **1202**, 113305 (2021).
40. M. U. Khan, J. Iqbal, M. Khalid, R. Hussain, A. A. C. Braga, M. Hussain and S. Muhammad, Designing triazatruxene-based donor materials with promising photovoltaic parameters for organic solar cells, RSC Adv., **9**, 26402–26418 (2019).
41. I. Kim, J. W. Lee, R. H. Jeong and J. H. Boo, A high-efficiency and stable perovskite solar cell fabricated in ambient air using a polyaniline passivation layer, Sci. Rep., **12**, 697 (2022).
42. A. Klamt, C. Moya and J. Palomar, A comprehensive comparison of the IEFPCM and SS (V) PE continuum solvation methods with the COSMO approach, J. Chem. Theory Comput., **11**, 4220–4225 (2015).
43. K. S. Liao, S. D. Yambem, A. Haldar, N. J. Alley and S. A. Curran, Designs and architectures for the next generation of organic solar cells, Energies., **3**, 1212–1250 (2010).
44. Y. Lin and X. Zhan, Designing efficient non-fullerene acceptors by tailoring extended fused-rings with electron-deficient groups, Adv. Energy Mater., **5**, 1501063 (2015).
45. Y. Lin, M. I. Nugraha, Y. Firdaus, A. D. Scaccabarozzi, F. Anies, A. H. Emwas and T. D. Anthopoulos, A simple n-dopant derived from diquat boosts the efficiency of organic solar cells to 18.3%, ACS Energy Lett., **5**, 3663–3671 (2020).
46. S. J. Lind, K. C. Gordon, S. Gambhir and D. L. Officer, A spectroscopic and DFT study of thiophene-substituted metalloporphyrins as dye-sensitized solar cell dyes, Phys. Chem. Chem. Phys., **11**, 5598–5607 (2009).
47. T. Liu, Y. Zhang, Y. Shao, R. Ma, Z. Luo, Y. Xiao and Y. Li, Asymmetric acceptors with fluorine and chlorine substitution for organic solar cells toward 16.83% efficiency, Adv. Funct. Mater., **30**, 2000456 (2020).
48. X. Q. Liu, C. F. Qin, N. D. Chen, J. W. Hao, S. T. Ma, M. Zhang and S. Li, Simultaneous determination of phenols in the four main original plants of the famous traditional Chinese medicine Shihu by pressurized capillary electrochromatography, RSC Adv., **13**, 19455–19463 (2023).
49. C. Lu, M. Paramasivam, K. Park, C. H. Kim and H. K. Kim, Phenothiazine functionalized multifunctional A–π–D–π–D–π–A type hole-transporting materials via sequential C–H arylation approach for efficient and stable perovskite solar cells, ACS Appl. Mater. Interfaces., **11**, 14011–14022 (2019).
50. T. Lu, Multiwfn, Version 2014 (2014).
51. H. Luo, J. Lai, C. Wang and Q. Chen, Understanding the effects of the energy band

alignment at the donor/acceptor interface on the open circuit voltage of organic photovoltaic devices, Chem. Phys. Lett., **711**, 113–117 (2018).
52. N. Maqsood, A. Asif, A. Elmushyakhi, M. Ans, R. A. Shehzad, A. Rasool and J. Iqbal, Environmentally affable and highly efficient donor material based on cyclopentadithiophene framework for remarkable organic solar cells, Opt. Mater., **135**, 113316 (2023).
53. N. Maqsood, A. Asif, M. Ans, Q. S. Hameed, A. Elmushyakhi, A. M. Shawky and J. Iqbal, Molecular engineering of bicarbazole-based donor molecules with remarkable photovoltaic parameters for organic solar cells, Optik., **281**, 170818 (2023).
54. M. Y. Mehboob, R. Hussain, M. U. Khan, M. Adnan, A. Umar, M. U. Alvi and M. N. Shahi, Designing N-phenylaniline-triazol configured donor materials with promising optoelectronic properties for high-efficiency solar cells, Comput. Theor. Chem., **1186**, 112908 (2020).
55. M. Y. Mehboob, R. Hussain, Z. Irshad and M. Adnan, Enhancement in the photovoltaic properties of hole transport materials by end-capped donor modifications for solar cell applications, Bull. Korean Chem. Soc., **42**, 597–610 (2021).
56. M. Y. Mehboob, R. Hussain, M. U. Khan, M. Adnan, M. A. Ehsan, A. Rehman and M. R. S. A. Janjua, Quantum chemical design of near-infrared sensitive fused ring electron acceptors containing selenophene as π-bridge for high-performance organic solar cells, J. Phys. Org. Chem., **34**, e4204 (2021).
57. M. Y. Mehboob, R. Hussain, M. U. Khan, M. Adnan, M. U. Alvi, J. Yaqoob and M. Khalid, Efficient designing of half-moon-shaped chalcogen heterocycles as non-fullerene acceptors for organic solar cells, J. Mol. Model., **28**, 125 (2022).
58. N. Naeem, R. A. Shehzad, M. Ans, M. S. Akhter and J. Iqbal, Dopant free triphenylamine-based hole transport materials with excellent photovoltaic properties for high-performance perovskite solar cells, Energy Technol., **10**, 2100838 (2022).
59. K. Okuno, Y. Shigeta, R. Kishi, H. Miyasaka and M. Nakano, Tuned CAM-B3LYP functional in the time-dependent density functional theory scheme for excitation energies and properties of diarylethene derivatives, J. Photochem. Photobiol. A Chem., **235**, 29–34 (2012).
60. J. Pastuszak and P. Węgierek, Photovoltaic cell generations and current research directions for their development, Materials., **15**, 5542 (2022).
61. A. Qundeel, M. Adnan, R. Hussain, R. A. Shehzad, S. Muhammad, G. Mustafa and Z. Irshad, Impact of end-capped engineering on the optoelectronic characteristics of pyrene-based non-fullerene acceptors for organic photovoltaics, Int. J. Quantum Chem., **124**, e27344 (2024).
62. A. Rafiq, R. Hussain, M. U. Khan, M. Y. Mehboob, M. Khalid, Shehnaz and K. Ayub, Novel star-shaped benzotriindole-based nonfullerene donor materials: toward the development of promising photovoltaic compounds for high-performance organic solar cells, Energy Technol., **10**, 2100751 (2022).
63. U. Rashid, J. Iqbal, M. I. Khan, Y. A. El-Badry, K. Ayub and R. A. Khera, Synergistic end-capped engineering on non-fused thiophene ring-based acceptors to enhance the photovoltaic properties of organic solar cells, RSC Adv., **12**, 12321–12334 (2022).
64. A. Rasool, M. Ans, L. A. El Maati, S. A. Abdelmohsen, B. M. Alotaibi and J. Iqbal, Designing of anthracene-arylamine hole transporting materials for organic and perovskite solar cells, J. Mol. Graph. Model., **122**, 108464 (2023).
65. A. Rasool, B. Basha, A. Elmushyakhi, I. Hossain, A. ur Rehman and M. Ans, Tuning the optoelectronic properties of acridine-triphenylamine (ACR-TPA) based novel hole transporting material for high efficiency perovskite and organic solar cell, J. Mol. Graph. Model., **123**, 108526 (2023).
66. S. Sadiq, M. Waqas, A. Zahoor, R. F. Mehmood, M. Essid, Z. Aloui and S. J. Akram, Synergistic modification of end groups in quinoxaline fused core-based acceptor molecule to enhance its photovoltaic characteristics for superior organic solar cells, J. Mol. Graph. Model., **123**, 108518 (2023).
67. H. Sajid, K. Ayub, M. A. Gilani and T. Mahmood, Donor-π-acceptor N-methyl-4,5-diazacarbazole based ultra-high performance organic solar cells: a density functional theory study, Energy Technol., **11**, 2201164 (2023).
68. R. Saleem, A. Farhat, R. A. Khera, P. Langer and J. Iqbal, Designing of small molecule non-fullerene acceptors with cyanobenzene core for photovoltaic application, Comput. Theor. Chem., **1197**, 113154 (2021).
69. M. C. Scharber and N. S. Sariciftci, Efficiency of bulk-heterojunction organic solar cells, Prog. Polym. Sci., **38**, 1929–1940 (2013).
70. M. C. Scharber, D. Muhlbacher, M. Koppe, P. Denk, C. Waldauf, A. J. Heeger and C. J. Brabec, Design rules for donors in bulk-heterojunction

solar cells—towards 10% energy-conversion efficiency, Adv. Mater., **18**, 789–794 (2006).
71. C. Scherelis, I. Penesis, M. A. Hemer, R. Cossu and J. T. Wright, Dataset for concurrent echosounder and ADCP measurements at a tidal energy candidate site in Australia, Data Brief., **31**, 105873 (2020).
72. R. Sharafat, A. Basharat, U. Salma, J. Iqbal, R. A. Khera, I. A. Shaaban and L. A. El Maati, Investigating the impact of end-capped acceptor alterations to dimethyl fluorene-based hole transporting material for perovskite solar cells, J. Phys. Chem. Solids., **186**, 111798 (2024).
73. A. Sharif, S. Jabeen, S. Iqbal and J. Iqbal, Tuning the optoelectronic properties of dibenzochrysene (DBC) based small molecules for organic solar cells, Mater. Sci. Semicond. Process., **127**, 105689 (2021).
74. C. Shen, Y. Wu, H. Zhang, E. Li, W. Zhang, X. Xu and W. H. Zhu, Semi-locked tetrathienylethene as a building block for hole-transporting materials: toward efficient and stable perovskite solar cells, Angew. Chem. Int. Ed., **58**, 3784–3789 (2019).
75. W. Shen, Y. Zhao and F. Liu, Highlights of mainstream solar cell efficiencies in 2023, Front. Energy., **18**, 8–15 (2024).
76. S. A. Siddique, M. B. A. Siddique, R. Hussain, X. Liu, M. Y. Mehboob, Z. Irshad and M. Adnan, Efficient tuning of triphenylamine-based donor materials for high-efficiency organic solar cells, Comput. Theor. Chem., **1191**, 113045 (2020).
77. H. J. Snaith, Present status and future prospects of perovskite photovoltaics, Nat. Mater., **17**, 372–376 (2018).
78. L. Sun, Y. Chen, M. Sun and Y. Zheng, Organic solar cells: physical principle and recent advances, Chem. Asian J., **18**, e202300006 (2023).
79. R. Sun, Y. Wu, X. Yang, Y. Gao, Z. Chen, K. Li and J. Min, Single-junction organic solar cells with 19.17% efficiency enabled by introducing one asymmetric guest acceptor, Adv. Mater., **34**, 2110147 (2022).
80. X. Sun, F. Wu, C. Zhong, L. Zhu and Z. A. Li, A structure–property study of fluoranthene-cored hole-transporting materials enables 19.3% efficiency in dopant-free perovskite solar cells, Chem. Sci., **10**, 6899–6907 (2019).
81. A. Tajammal, M. Ans, R. F. Mehmood, J. Iqbal, S. J. Akram, A. Murtaza and R. A. Khera, Engineering of A2-D-A1-D-A2 type BT-dIDT based non-fullerene acceptors for effective organic solar cells, Comput. Theor. Chem., **1211**, 113666 (2022).
82. S. Tang and J. Zhang, Design of donors with broad absorption regions and suitable frontier molecular orbitals to match typical acceptors via substitution on oligo(thienylenevinylene) toward solar cells, J. Comput. Chem., **33**, 1353–1363 (2012).
83. M. Thomas, M. Y. Darensbourg and M. B. Hall, Computational definition of a mixed valent Fe(II)Fe(I) model of the [FeFe] hydrogenase active site resting state, J. Inorg. Biochem., **101**, 1752–1757 (2007).
84. G. Tunc, E. Guzel, I. Sisman, V. Ahsen, G. Cardenas-Jiron and A. G. Gurek, Effect of new asymmetrical Zn(II) phthalocyanines on the photovoltaic performance of a dye-sensitized solar cell, New J. Chem., **43**, 14390–14401 (2019).
85. M. Vasiliev, M. Nur-E.-Alam and K. Alameh, Recent developments in solar energy-harvesting technologies for building integration and distributed energy generation, Energies., **12**, 1080 (2019).
86. S. N. Villadsen, P. L. Fosbol, I. Angelidaki, J. M. Woodley, L. P. Nielsen and P. Møller, The potential of biogas; the solution to energy storage, ChemSusChem., **12**, 2147–2153 (2019).
87. W. Wang, X. Miao, G. Cai, L. Ding, Y. Li, T. Li and Y. Lin, Enhancing transition dipole moments of heterocyclic semiconductors via rational nitrogen-substitution for sensitive near infrared detection, Adv. Mater., **34**, 2201600 (2022).
88. M. Waqas, N. M. A. Hadia, A. M. Shawky, R. F. Mahmood, M. Essid, Z. Aloui and R. A. Khera, Theoretical framework for achieving high Voc in non-fused non-fullerene terthiophene-based end-capped modified derivatives for potential applications in organic photovoltaics, RSC Adv., **13**, 7535 (2023).
89. H. Yao, L. Ye, H. Zhang, S. Li, S. Zhang and J. Hou, Molecular design of benzodithiophene-based organic photovoltaic materials, Chem. Rev., **116**, 7397 (2016).
90. X. Yin, Z. Song, Z. Li and W. Tang, Toward ideal hole transport materials: a review on recent progress in dopant-free hole transport materials for fabricating efficient and stable perovskite solar cells, Energy Environ. Sci., **13**, 4057 (2020).
91. F. Younas, M. Y. Mehboob, K. Ayub, R. Hussain, A. Umar, M. U. Khan and M. Adnan, Efficient Cu decorated inorganic B12P12 nanoclusters for sensing toxic COCl2 gas: a detailed DFT study, J. Comput. Biophys. Chem., **20**, 85 (2021).

92. W. A. Zahid, W. Akram, M. F. Ahmad, S. Iqbal, S. A. Abdelmohsen, M. M. Alanazi and J. Iqbal, Designing of phenothiazine-based hole-transport materials with excellent photovoltaic properties for high-efficiency perovskite solar cells (PSCs), Spectrochim. Acta A Mol. Biomol. Spectrosc., **298**, 122774 (2023).
93. Z. Zara, J. Iqbal, S. Bibi, S. Sadaf and B. Eliasson, Designing benzodithiophene-based donor materials with favorable photovoltaic parameters for bulk heterojunction organic solar cells, ChemistrySelect., **2**, 5628 (2017).
94. L. Zhang, X. Zhou, C. Liu, X. Wang and B. Xu, A review on solution-processable dopant-free small molecules as hole-transporting materials for efficient perovskite solar cells, Small Methods., **4**, 2000254 (2020).
95. J. Zhou, X. Wan, Y. Liu, G. Long, F. Wang, Z. Li and Y. Chen, A planar small molecule with dithienosilole core for high efficiency solution-processed organic photovoltaic cells, Chem. Mater., **23**, 4666 (2011).
96. H. Zubair, M. S. Akhter, M. Waqas, M. Ishtiaq, I. A. Bhatti, J. Iqbal and R. A. Khera, A computational insight into enhancement of photovoltaic properties of non-fullerene acceptors by end-group modulations in the structural framework of INPIC molecule, J. Mol. Graph. Model., **126**, 108664 (2024).